CLASSIFICATION OF BREAST DENSITY IN X-RAY MAMMOGRAPHY

Václav Remeš *Michal Haindl*

The Institute of Information Theory and Automation of the Czech Academy of Sciences
Department of Pattern Recognition
{remes,haindl}@utia.cas.cz

ABSTRACT

Breast density is an important cue to detect both the presence of suspicious cancerous masses and to predict future possibility for cancer development. A fast breast density classification method is presented and successfully tested on two state-of-the-art mammogram databases. The X-ray digital mammogram tissue texture is locally represented by the two-dimensional adaptive causal autoregressive spatial model and its parameters are used as the classification features.

***Index Terms*—** Mammography, ACR, BI-RADS, MRF, breast density

1. INTRODUCTION

Breast cancer is the most common type of cancer among middle-aged women in most developed countries [1, 2]. Almost one woman in ten grows a breast cancer in her life. To lower the mortality rate, women in the developed countries usually regularly attend a preventive mammography screening. Although the X-ray mammography is sensitive in screening and diagnosis of breast cancer, it suffers from a high false-positive (FP) rate [3]. Mammographic breast density is very important but one of the most undervalued and underused risk factors in studies investigating breast cancer occurrence. The risk of breast cancer is four to six times higher for women with dense breasts [4]. Breast density may also decrease the sensitivity by up to 40 % [4], obscure tumors, or mimic breast cancer, and, thus, the accuracy of mammography. An increase in breast density can also be used to characterize the effects of hormone replacement therapy. Thus many papers [5, 6, 7, 8, 9, 10, 11] consider automatic breast density classification using different approaches in feature extraction, used classifiers, and tested databases.

1.1. ACR BI-RADS

American College of Radiology (ACR) Breast Imaging Reporting and Data System (BI-RADS) [12] classifies breast density into the following 4 groups:

978-1-4673-8457-5/15/$31.00

BI-RADS I The breast is almost entirely fat, fibrous and glandular tissue makes up less than 25% of the breast.

BI-RADS II There are scattered fibroglandular densities. Fibrous and glandular tissue makes up from 25 to 50% of the breast.

BI-RADS III The breast tissue is heterogeneously dense and the breast has more areas of fibrous and glandular tissue (from 51 to 75%) that are found throughout the breast. This can make it hard to see small masses (cysts or tumors).

BI-RADS IV The breast tissue is extremely dense. The breast is made up of more than 75% fibrous and glandular tissue. This can lead to missing some cancers.

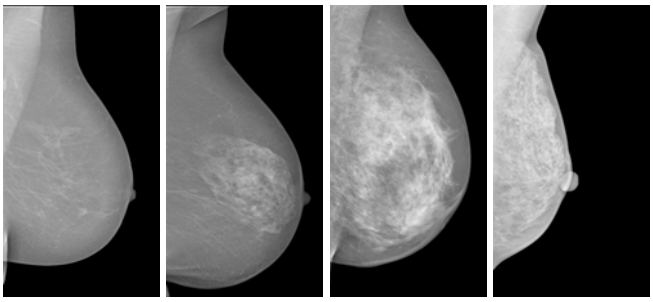

Fig. 1. Example mammograms with different density values - left to right consequently contain BI-RADS I, II, III and IV. Images from the INbreast database

2. MRF TEXTURE MODEL

The mammography tissue textures in the form of monospectral images are locally modeled by their dedicated directional Gaussian noise-driven autoregressive random field two-dimensional model (2DCAR), because this model has good modeling performance, is very fast and allows analytical treatment [13, 14]. The 2DCAR random field is a Markovian family of random variables with a joint probability density on the set of all possible realizations Y of the

$M \times N$ lattice I, subject to the following condition:

$$p(Y \mid \gamma_\phi, \sigma_\phi^{-2}) = (2\pi\sigma_\phi^2)^{-\frac{(MN-1)}{2}} \exp\left\{\frac{-1}{2} tr\left\{\sigma_\phi^{-2}\begin{pmatrix}-\alpha\\ \gamma_\phi^T\end{pmatrix}^T \tilde{V}_{MN-1}\begin{pmatrix}-\alpha\\ \gamma_\phi^T\end{pmatrix}\right\}\right\} , \quad (1)$$

where α is a unit vector, $tr()$ is a trace of the corresponding matrix, and the following notation is used:

$$\tilde{V}_{r-1} = \sum_{k=1}^{r-1}\begin{pmatrix}Y_k Y_k^T & Y_k X_k^T\\ X_k Y_k^T & X_k X_k^T\end{pmatrix} = \begin{pmatrix}\tilde{V}_{y(r-1)} & \tilde{V}_{xy(r-1)}^T\\ \tilde{V}_{xy(r-1)} & \tilde{V}_{x(r-1)}\end{pmatrix} .$$

Here, $r = [r_1, r_2, \phi]$ is spatial multiindex denoting the history of movements on the rectangular lattice I, where r_1, r_2 are row and column indices, and the possible model development directions are $\phi \in \{0°, 45°, 90°, 135°, 180°, 225°, 270°, 315°\}$. The 2DCAR model can be expressed as a stationary causal uncorrelated noise-driven 2D autoregressive process:

$$Y_r = \gamma_\phi X_r + e_r , \quad (2)$$

where $\gamma_\phi = [a_1, \ldots, a_\eta]$ is the parameter vector, X_r is a support vector of $[Y_{r-{}^1s}, \ldots, Y_{r-{}^\eta s}]^T$ where ${}^i s \in I_r^c$. I_r^c denotes a causal (or alternatively unilateral) contextual neighborhood (i.e., all the support pixels were previously visited and thus their values are known), and $\eta = cardinality(I_r^c)$. Furthermore, e_r denotes white Gaussian noise with zero mean and a constant but unknown variance σ^2.

The method uses a locally adaptive version of this 2DCAR model [13], where its recursive statistics are modified by an exponential forgetting factor, i.e., a constant smaller than 1 which is used to weight the older data.

Parameter estimation of the 2DCAR model using either the maximum likelihood, or the least square or Bayesian methods can be found analytically. The Bayesian parameter estimates of the 2DCAR model using the normal-gamma parameter prior are:

$$\begin{aligned}\hat{\gamma}_{r-1}^T &= V_{x(r-1)}^{-1} V_{xy(r-1)} , \quad (3)\\ V_{(r-1)} &= \tilde{V}_{(r-1)} + V_{(0)} ,\\ \beta(r) &= \beta(0) + r - 1 ,\end{aligned}$$

and $\beta(0)$ is an initialization constant and sub-matrices in $V_{(0)}$ are from the parameter prior. The parameter estimate (3) can also be evaluated recursively ([13]).

3. CLASSIFICATION SCHEME

For breast density classification we use supervised classification. In both the training and classification steps the breast area has to be first identified in the image. With fully digital databases (INbreast), this step is very simple – breast pixels are usually only those with value greater than 0.

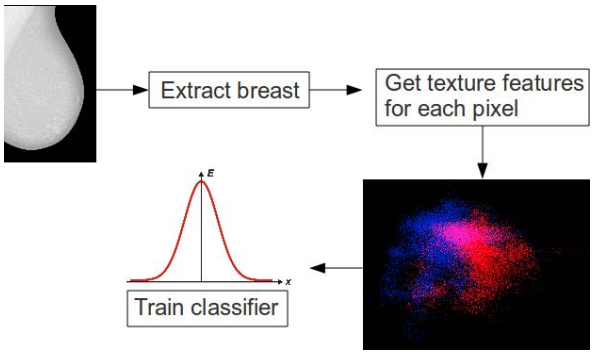

Fig. 2. Classifier training

Digitised databases commonly contain lots of noise and also mostly have some labels scanned in the mammograms. To extract the breast area we first apply a median filter on the image to reduce noise and then use adaptive thresholding to extract non-background areas. The breast is then selected as the biggest non-background area. For performance efficiency we also downscale the images to 400 px height keeping the aspect ratio.

3.1. Classifier training

The classifier is trained as indicated in Fig. 2. After the breast area has been segmented from the image, we extract the feature vectors θ for each pixel $\theta = \{\gamma_{\phi_1}, \gamma_{\phi_2}, ...\}$. The model directions used are $\phi_i \in \{90°, 135°, 180°, 315°\}$, for which we observed the best results. We use the maximum-likelihood classifier based on the multivariate Gaussian distribution:

$$f(X|C) = \frac{1}{\sqrt{(2\pi)^k |\Sigma_C|}} e^{\left(-\frac{1}{2}(\theta-\mu_C)^T \Sigma_C{}^{-1}(\theta-\mu_C)\right)} \quad (4)$$

where C is the BI-RADS density value of the particular mammogram. μ_C is the mean value of class C and Σ_C is the corresponding covariance matrix.

This way we estimate the feature distribution of each BI-RADS class. We presume that even though the ACR BI-RADS density description specifies the different classes based on the ratio of fatty and dense areas in the breast, our texture model is able to distinguish between fatty, heterogeneous, mostly dense and dense textures. Thus we can train the texture models as if the heterogeneity is a kind of texture within the breast.

3.1.1. Feature space visualisation

To confirm the correctness of our chosen texture model for the application of breast texture modeling, we visualised the feature space, distinguishing the different density types with the colour of the pixels. We extracted the feature values for all the pixels of different breasts and applied the Karhunen-Loeve

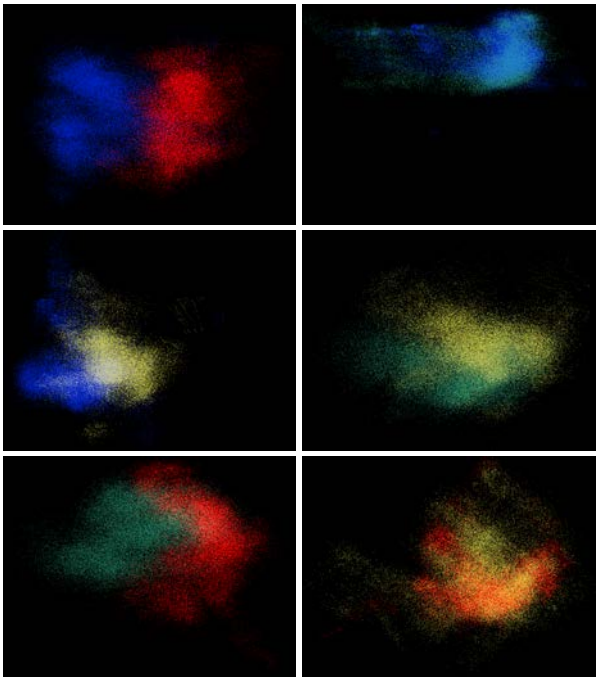

Fig. 3. Features from INbreast data and class combinations (rightwards, top to bottom) 1x4, 1x2, 1x3, 2x3, 2x4, 3x4

transform, taking values of the 2 most significant components as the x and y coordinates of the features to be displayed.

We can see in Fig. 3 that our model distinguishes the different density textures fairly well with best results being between the most distant classes. This is indeed logical since closer classes have more similar textures.

3.2. Breast density classification

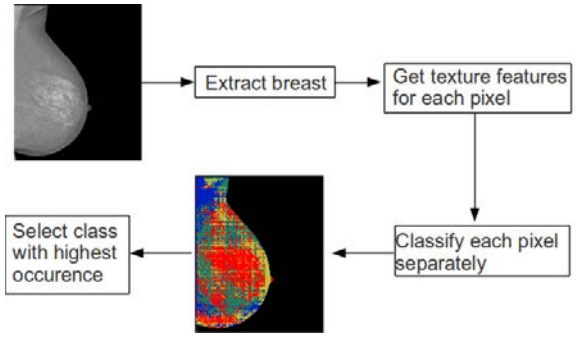

Fig. 4. Classification

We classify the mammograms into the different density categories as shown in Fig. 4. We first extract the feature vectors for each pixel as described in Sec. 3.1 and then for each pixel compute the likelihood for each density class (4). The pixel is then assigned the class with highest likelihood. We can see in the example in Fig. 5 that the different texture types are reasonably assigned with the dense area clearly marked in red colour. The whole breast is then classified according to the pixel majority class.

Table 1. INbreast database classification results for all double-class combinations and the complete four BI-RADS tissue classes (rows $\sim$ references, columns $\sim$ interpretation).

1x4	**1**	**2**	**3**	**4**	**Sensitivity**
1	132	0	0	4	97%
2	88	0	0	59	0.0%
3	23	0	0	76	0.0%
4	2	0	0	26	92.8%
Precision	98.5%			86.7%	
1x3, **1**	128	0	8	0	94.1%
2	81	0	66	0	0.0%
3	15	0	84	0	84.8%
4	4	0	24	0	0.0%
Precision	88.3%		91.3%		
1x2, **1**	80	56	0	0	58.8%
2	20	127	0	0	86.4%
3	7	92	0	0	0.0%
4	0	28	0	0	0.0%
Precision	80%	69.4%			
2x4, **1**	0	133	0	3	0.0%
2	0	137	0	10	93.2%
3	0	60	0	39	0.0%
4	0	4	0	24	85.7%
Precision		97.2%		70.6%	
2x3, **1**	0	132	4	0	0.0%
2	0	122	25	0	83.0 %
3	0	33	66	0	66.7%
4	0	6	22	0	0.0%
Precision		78.7%	72.5%		
3x4, **1**	0	0	96	40	0.0%
2	0	0	118	29	0.0 %
3	0	0	89	10	89.9%
4	0	0	14	14	50.0%
Precision			86.4%	58.3%	
1x2x3x4, **1**	95	23	18	0	69.9%
2	33	60	49	5	40.8%
3	6	19	58	16	58.6%
4	0	7	3	18	64.3%
Precision	70.9%	55%	45.3%	46.2%	

4. MAMMOGRAM DATABASES

The INbreast database [15] is a mammographic database, with images acquired at a Breast Centre, located in a University Hospital (Hospital de São João, Breast Centre, Porto,

Table 2. MIAS database, all dichotomous and one classification result for all three (fatty, fatty-glandular, dense-glandular) tissue classes (rows $\sim$ references, columns $\sim$ interpretation).

1x3	**1**	**2**	**3**	**Sensitivity**
1	92	0	12	88.5%
2	33	0	70	0.0 %
3	5	0	106	95.5%
Precision	94.8%		89.8%	
1x2, **1**	72	32	0	69.2%
2	10	93	0	90.3 %
3	2	109	0	0.0%
Precision	87.8%	74.4%		
2x3, **1**	0	104	0	0.0%
2	0	95	8	92.2 %
3	0	57	54	48.6%
Precision		62.5%	87.1%	
1x2x3, **1**	89	8	7	85.6%
2	20	57	26	55.3 %
3	8	34	69	62.2%
Precision	76.1%	57.6%	67.6%	

Portugal). INbreast has a total of 115 cases (410 - 8Mpix, 12bit gray-scale DICOM images) of which 90 cases are from women with both breasts (4 images per case) and 25 cases are from mastectomy patients (2 images per case).

The Mammographic Image Analysis Society Digital Mammogram Database (MIAS) [16] is a database with 322 medio-lateral oblique (MLO) 1024×1024 images digitized to 50 microns per pixel from the original X-ray film-screen mammograms. MIAS uses its own density description - fatty ($\sim$ BI-RADS I), fatty-glandular ($\sim$ BI-RADS II-III), dense-glandular ($\sim$ BI-RADS III-IV).

5. RESULTS

The comparative experimental results were tested on the MIAS database [16] and on the state-of-the-art public digital mammogram INbreast database [15]. We tested the classification of all the possible pairs of classes to see the limits of our method. We also tested the classification of all the classes together. For each tested case we selected 5 random mammograms for each class as training data and classified the rest of the database (excluding training images). The results can be seen in Tabs. 1, 2. Value at i-th row and j-th column means the number of times a mammogram of class i was classified as class j. The top-left cell of each table shows which classes have been classified against each other.

The results for the MIAS database seem a little more precise than for the INbreast database. This can be caused by the fact that the MIAS database doesn't provide the density information according to the ACR BI-RADS standard but rather

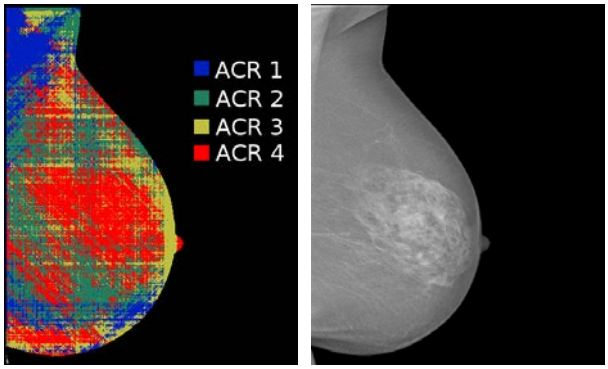

Fig. 5. Example of pixel classification into different density classes

provides its own method with 3 classes instead of 4. There are no alternative tissue classification results for the INbreast database, so we compare our results with the state-of-the-art methods applied to the obsolete MIAS data.

Muhimmah and Zwiggelaar [8] obtained slightly better results ($\langle 63; 91 \rangle \%$) sensitivity and precision ($\langle 74; 80 \rangle \%$) for their best multiresolution histogram features-based published method and ($\langle 57; 83 \rangle \%$) sensitivity and precision ($\langle 54; 75 \rangle \%$) for the single resolution variant on the MIAS database. Both methods use the Directed Acyclic Graph - Support Vector Machine (DAG-SVM) classifier. However, the multiresolution method uses fifty times more features than our method and the single resolution method is worse than our presented single resolution method. Mustra et al. [11] has the best published results - ($\langle 75; 87 \rangle \%$) sensitivity and precision ($\langle 74; 91 \rangle \%$) on MIAS to our knowledge. They need fifteen times more features than we do, use slow k-NN classifier, and while we learn the classifier on just five images per class, they use the whole database of 321 images (leave-one-out).

6. CONCLUSION

We have presented a novel method for breast density classification in X-ray mammography. The method was tested on the widely known, yet a little obsolete, MIAS database and the state-of-the art INbreast database, and our preliminary results are promising and competitive. Furthermore, the intermediate results of our method can be used for preliminary breast tissue type classification. In the future, we plan to extend the classification part with a more complex classifier than a max-likelihood multivariate Gaussian, incorporate a sophisticated preprocessing step and use the multiresolution approach.

Acknowledgements

This research was supported by the Czech Science Foundation project GAČR 14-10911S.

7. REFERENCES

[1] Tiffany Tweed and Serge Miguet, "Automatic detection of regions of interest in mammographies based on a combined analysis of texture and histogram," in *Pattern Recognition, 2002. Proceedings. 16th International Conference on*, Los Alamitos, CA, USA, 2002, vol. 2, pp. 448–452, IEEE Computer Society.

[2] Hairong Qi and Nicholas A. Diakides, "Thermal infrared imaging in early breast cancer detection - a survey of recent research," in *Proceedings of the 25th Annual International Conference of the IEEE Engineering in Medicine and Biology Society*. IEEE, 2003, vol. 2, pp. 1109–1112.

[3] Naga R. Mudigonda, Rangaraj M. Rangayyan, and J. E. Leo Desautels, "Detection of breast masses in mammograms by density slicing and texture flow-field analysis," *IEEE Trans. Med. Imaging*, vol. 20, no. 12, pp. 1215–1227, 2001.

[4] Patricia A. Carney, Diana L. Miglioretti, Bonnie C. Yankaskas, Karla Kerlikowske, Robert Rosenberg, Carolyn M. Rutter, Berta M. Geller, Linn A. Abraham, Steven H. Taplin, Mark Dignan, Gary Cutter, and Rachel Ballard-Barbash, "Individual and combined effects of age, breast density, and hormone replacement therapy use on the accuracy of screening mammography," *Annals of Internal Medicine*, vol. 138, no. 3, pp. 168–175, 2003.

[5] Nico Karssemeijer, "Automated classification of parenchymal patterns in mammograms," *Physics in medicine and biology*, vol. 43, no. 2, pp. 365, 1998.

[6] Keir Bovis and Sameer Singh, "Classification of mammographic breast density using a combined classifier paradigm," in *Medical Image Understanding and Analysis (MIUA) Conference, Portsmouth*. Citeseer, 2002.

[7] Arnau Oliver, Jordi Freixenet, and Reyer Zwiggelaar, "Automatic classification of breast density," in *Image Processing, 2005. ICIP 2005. IEEE International Conference on*. IEEE, 2005, vol. 2, pp. II–1258.

[8] Izzati Muhimmah and Reyer Zwiggelaar, "Mammographic density classification using multiresolution histogram information," in *Proceedings of the International Special Topic Conference on Information Technology in Biomedicine, ITAB*. Citeseer, 2006.

[9] Arnau Oliver, Jordi Freixenet, Robert Marti, Josep Pont, Ernesto Perez, Erika RE Denton, and Reyer Zwiggelaar, "A novel breast tissue density classification methodology," *Information Technology in Biomedicine, IEEE Transactions on*, vol. 12, no. 1, pp. 55–65, 2008.

[10] Albert Torrent, Anton Bardera, Arnau Oliver, Jordi Freixenet, Imma Boada, Miguel Feixes, Robert Martí, Xavier Lladó, Josep Pont, Elsa Pérez, et al., "Breast density segmentation: a comparison of clustering and region based techniques," in *Digital Mammography*, pp. 9–16. Springer, 2008.

[11] Mario Muštra, Mislav Grgić, and Krešimir Delač, "Breast density classification using multiple feature selection," *AUTOMATIKA: časopis za automatiku, mjerenje, elektroniku, računarstvo i komunikacije*, vol. 53, no. 4, pp. 362–372, 2012.

[12] American College of Radiology, BI-RADS Committee, et al., *ACR BI-RADS breast imaging and reporting data system: breast imaging atlas*, American College of Radiology, 2003.

[13] Michal Haindl, "Visual data recognition and modeling based on local markovian models," in *Mathematical Methods for Signal and Image Analysis and Representation*, Luc Florack, Remco Duits, Geurt Jongbloed, Marie-Colette Lieshout, and Laurie Davies, Eds., vol. 41 of *Computational Imaging and Vision*, chapter 14, pp. 241–259. Springer London, 2012, 10.1007/978-1-4471-2353-8_14.

[14] M. Haindl, "Texture synthesis," *CWI Quarterly*, vol. 4, no. 4, pp. 305–331, December 1991.

[15] Inês C Moreira, Igor Amaral, Inês Domingues, António Cardoso, Maria João Cardoso, and Jaime S Cardoso, "Inbreast: toward a full-field digital mammographic database," *Academic radiology*, vol. 19, no. 2, pp. 236–248, 2012.

[16] John Suckling, J Parker, DR Dance, S Astley, I Hutt, C Boggis, I Ricketts, E Stamatakis, N Cerneaz, Siew-Li Kok, et al., "The mammographic image analysis society digital mammogram database," in *2nd International Workshop on Digital Mammography*. 1994, International Congress Series, pp. 1069: 375–378, Excerta Medica.